

## PRECIPITATION VARIATIONS IN THE EASTERN PART OF THE HEXI CORRIDOR DURING AD 1765–2010 REVEAL CHANGING PRECIPITATION SIGNAL IN GANSU

FENG CHEN<sup>1</sup>, YU-JIANG YUAN<sup>1</sup>, RUI-BO ZHANG<sup>1</sup>, HUI-QIN WANG<sup>2</sup>, HUA-MING SHANG<sup>1</sup>,  
TONG-WEN ZHANG<sup>1</sup>, LI QIN<sup>1</sup>, and ZI-ANG FAN<sup>1</sup>

<sup>1</sup>Key Laboratory of Tree-Ring Physical and Chemical Research of China Meteorological Administration, Key Laboratory of Tree-Ring Ecology of Uigur Autonomous Region, Institute of Desert Meteorology, China Meteorological Administration, No 46 Jianguo Road, Urumqi, China

<sup>2</sup>College of Earth and Environmental Science, Lanzhou University, Lanzhou, China

### ABSTRACT

We reconstructed August–May precipitation from AD 1765 to 2010 for the eastern part of the Hexi Corridor, northwest China, using tree rings of *Picea crassifolia*. The precipitation reconstruction explains 44.1% of the actual precipitation variance during the common period of 1951–2010. The precipitation reconstruction is representative of precipitation conditions over a large area of the Hexi Corridor. Multi-taper spectral analysis reveals the existence of significant variability with periods of 9.3, 6.7, 3.1, and 2.6 years. Comparison between the precipitation reconstruction of the eastern part of the Hexi Corridor and other nearby precipitation/drought reconstructions shows high coherency in the timing of dry/wet episodes on annual to decadal scale. The divergences existing between the reconstructions may reflect the influence of different geographic features in Gansu and differences in seasonality of the various precipitation/drought reconstructions.

*Keywords:* dendrochronology, precipitation reconstruction, eastern part of the Hexi Corridor.

### INTRODUCTION

The Hexi Corridor in Gansu Province, which is surrounded by the Gobi Desert in the north and the Tibetan Plateau in the south, is one of the major agricultural production regions in west China. There are many fertile oases along the Qilian Mountains, watered by rivers, such as the Shiyang, Heihe and Shule Rivers, flowing from alpine regions. However, because of the lack of water resources, people in some areas of the Hexi Corridor are facing the consequences of some of the worst ecological and environmental deterioration, which has captured the attention of the Chinese government and the scientific community (Wang *et al.* 2002; Wang *et al.* 2004). Therefore, investigation of the hydroclimatic variations in the Hexi Corridor is a high research priority. However, the instrumental records of hydroclimatic variability in this area are very short, generally beginning in the 1960s. This limits the analysis of long-term hydroclimate trends from instrumental records. To better understand the long-term

climate history for proper water resource management and planning, we need detailed and reliable knowledge of the hydroclimatic conditions from high-resolution proxy data.

Climate-sensitive tree rings are one of most valuable and long-term sources of climate proxy data (Fritts 1976; Hughes *et al.* 2011). Dendroclimatologists have developed many tree-ring chronologies, particularly in the upper treeline and arid-semiarid areas of the Hexi Corridor. Recent reconstructions of precipitation, drought, and river streamflow based on tree-ring chronologies indicated that there is great potential in developing century-to-millennium length reconstructions of hydroclimatic variability over the Hexi Corridor (Liang *et al.* 2009; Chen *et al.* 2011, 2012, 2013a; Yang *et al.* 2011, 2012; Deng *et al.* 2013; Liu *et al.* 2013; Gou *et al.* 2014). However, to date, few studies have considered the analysis of precipitation of the eastern part of the Hexi Corridor in a long-term context.

Qin Hai spruce (*Picea crassifolia* Kom.), found at dry sites of the Hexi Corridor (Chen *et al.* 2011,

2013a), have shown utility for reconstructing annual precipitation variations. Previous studies have shown that the growth of Qinhai spruce is primarily influenced by annual rainfall, and climate variables explained up to 45% of the tree-ring width variance (Chen *et al.* 2011, 2013a). The purpose of this study was to reconstruct precipitation series for the eastern part of the Hexi Corridor based on tree-ring width data of Qinhai spruce. Furthermore, the agreement of the reconstructed annual rainfall with the documentary records and independent precipitation/drought reconstructions from western-central and eastern Gansu, which are based on tree-ring data, was evaluated.

## DATA AND METHODS

### Study Area

The study area is located in the eastern part of the Hexi Corridor between the Gobi Desert and the Tibetan Plateau. The climate is affected by the Westerlies and Asian summer monsoon, and characterized as arid continental. Mean annual precipitation is 165 mm and mean annual temperature is 8.1°C (climate data were provided by the Wuwei climate station). July is the hottest month (average temperature 22°C) and August is the wettest month (mean precipitation 38 mm). The cores of Qinghai spruce were collected from two sites (SJL and CLY) in the eastern part of the Hexi Corridor (Figure 1). SJL is located in the Qilian Mountains near the Tibetan Plateau, and CLY is located in the Changling Mountains near the Gobi Desert and has a large natural forest with little human disturbance (Table 1). The soil at both sites is thin and

rocky. The dominant tree species of the SJL site is Qinghai spruce and Qilian juniper (*Sabina przewalskii* Kom.). The dominant tree species of the CLY site are Chinese pine (*Pinus tabulaeformis* Carr.) and Qinghai spruce.

### Tree-Ring Data

In general, two increment cores were extracted from each tree. In combination, the two sites provided 97 increment cores taken from 51 trees. All cores were taken back to the Key Laboratory of Tree-Ring Physical and Chemical Research of the China Meteorological Administration. Air-dried cores were mounted on prefabricated wooden mounts and polished with sandpaper to enhance tree-ring boundaries. Tree-ring widths were measured to the nearest 0.001 mm with a TA Unislide Measurement System (Velmetx Inc., Bloomfield, New York). The program COFECHA helped to identify segments within each ring series showing erroneous crossdating and to correct mistakes (Holmes 1983). However, COFECHA does not replace manual (visual) crossdating. Thus, the statistical crossdating performed by COFECHA was always visually verified against the image loaded in the program Tree-ring Test (TT) (Chen *et al.* 2013a). The program TT in FORTRAN 90 was developed by Prof. Yuan Yujiang, and it can plot and edit tree-ring data on the screen.

The program ARSTAN (Cook 1985) was used to develop regional chronologies. Because of high mean correlation ( $r = 0.624$ ) of the individual cores with master series, all series of the two sites were applied to develop a regional chronology for the analysis. To reduce the undesirable growth

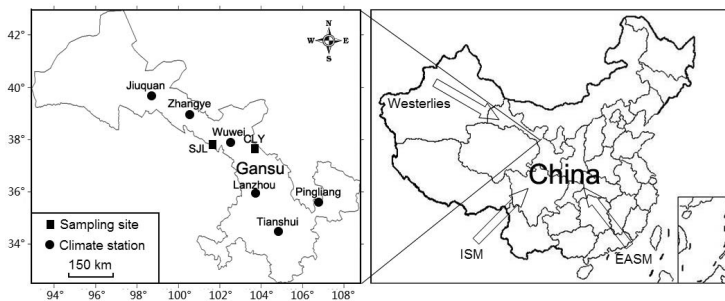


**Figure 1.** Location map of sampling sites and meteorological stations. ISM and EASM denote the Indian summer monsoon and the East Asian summer monsoon, respectively.

**Table 1.** Information about the sampling sites in the eastern part of the Hexi Corridor.

Site code	Latitude (N)	Longitude (E)	Elevation (m)	Aspect	Slope	Time span (A.D.)
SJL	37°52′20.82″	101°56′14.42″	2650	W	10–15°	1737–2010
CLY	37°26′39.85″	103°41′04.88″	2350	N	15–30°	1869–2010

trends related to non-climatic factors, such as increasing age and stand dynamics, each individual ring-width measurement series was first de-trended using a negative exponential curve in the ARSTAN program (Cook 1985). The de-trended series were then combined into regional chronologies using a bi-weight robust mean. Three versions of the tree-ring width chronology created by the ARSTAN program were Residual, Standard and Arstan. The residual tree-ring chronology was used in the further analyses. As is generally the case in tree-ring studies, sample depth within a chronology decreases back in time and may result in time-dependent variance changes and a weaker common signal in the earlier part of the chronology. Thus, an expressed population signal (EPS, Wigley et al. 1984) threshold of 0.85, which corresponds to a minimum sample depth of three trees, was used to assess the adequacy of the replications in the early years of the chronology. The chronology used in the precipitation reconstruction below was therefore truncated prior to 1765 based on the threshold values.

### Meteorological Data and Analysis Methods

The monthly precipitation and temperature records from the Wuwei climate station were used in this study. The Wuwei climate station is located at 102°40′E, 37°55′N, 1531.9 m a.s.l., and its records date from 1951 to 2010. Figure 2 shows the average monthly precipitation and temperature from 1951 to 2010 at the Wuwei climate station. The tree-ring index was compared with a 15-month window of climate data spanning the period from the previous July through September of the current growing season. To determine the most appropriate model for climate reconstruction, we also correlated the tree-ring index with seasonal combinations of climate data.

A linear regression equation between the predictand (climate factors) and the predictors (tree-ring index) was computed for the calibration

period. Split-sample calibration-verification tests were employed to evaluate the statistical fidelity of the reconstruction model (Meko and Graybill 1995). The testing statistics used included the reduction of error (RE) and coefficient of efficiency (CE) statistics, the sign test, the first-order sign test and Pearson correlation coefficient. Spectral analysis was performed using a multi-taper method (Mann and Lees 1996). To extract the common variations from the networks of tree-ring sites in Gansu, principal component analyses (PCA) was applied over the common period.

## RESULTS AND DISCUSSION

### Correlations with Climate and Precipitation Reconstruction

Figure 3 shows the correlations between the residual chronology and monthly climate records in our study area. Generally, the precipitation shows significant correlations with tree-ring widths, which indicates that low rates of precipitation in these months (August and September of the previous year, and March of the current year) limited the size of the tree rings. Correlations between tree-ring width index and mean temperatures are

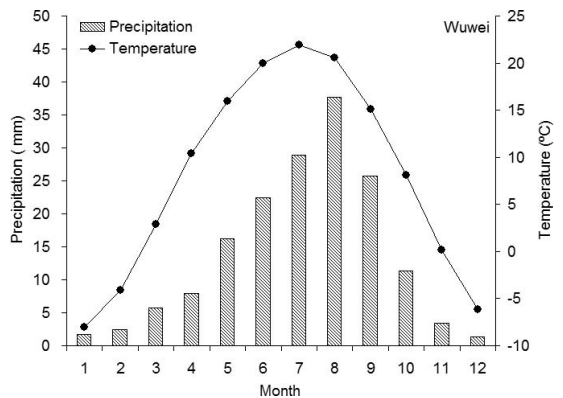


**Figure 2.** Average monthly precipitation and temperature values from 1951 to 2010 at the Wuwei meteorological station.

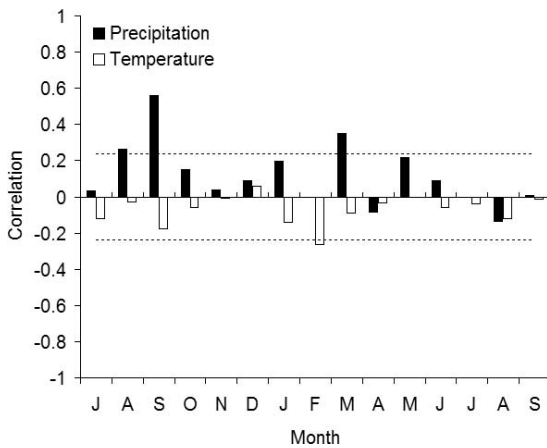


**Figure 3.** Correlation analysis between tree-ring width indices and meteorological data. Horizontal lines are at the 95% confidence level.

not significant (with the exception of February of the current year). As seasonally averaged climate data are more representative of climate conditions than data of a single month (Tian *et al.* 2007), different seasonal combinations of climate data were tested for climate reconstruction. The highest correlation between tree rings and the seasonalized precipitation was found in August–May ( $r = 0.664$ ,  $p < 0.001$ ). Therefore, the reconstruction was performed by calibrating tree rings with total August–May precipitation data. As shown in Table 2, the calibration and verification results for the split subperiods, *i.e.* 1951–1980 and 1981–2010, generally showed a good model fit. The reconstruction explained 44.1% of the actual precipitation variance during 1951–2010 (Figure 4).

### Characteristics of the Precipitation Reconstruction

The reconstructed and low-pass filtered total August–May precipitation for the eastern part of

the Hexi Corridor is presented in Figure 5. The long-term mean of the precipitation reconstruction based on regression is 111.8 mm for the period AD 1765–2010 and the standard deviation ( $\sigma$ ) is 19.8 mm. The thick line in Figure 5 is the 11-year low-pass filtered total August–May precipitation reconstruction. The reconstruction series includes eleven dry periods (precipitation  $< 111.8$  mm), including AD 1773 to 1784, 1791 to 1803, 1813 to 1823, 1831 to 1864, 1876 to 1886, 1909 to 1918, 1926 to 1932, 1949 to 1953, 1957 to 1960, 1987 to 1992 and 1998 to 2001, and four wet periods (precipitation  $> 111.8$  mm), including AD 1765 to 1772, 1785 to 1790, 1804 to 1812, 1824 to 1830, 1865 to 1875, 1887 to 1908, 1919 to 1925, 1933 to 1948, 1954 to 1956, 1961 to 1986, 1993 to 1997 and 2002 to 2010. We defined a dry year as having precipitation less than the mean  $-1\sigma$  (92.0 mm), and a wet year as having precipitation greater than the mean  $+1\sigma$  (131.6 mm).

Forty-one years were categorized as dry years and 38 years were classified as wet years during the last 246 years. According to observations, the drought in AD 1957 was the most serious drought in the eastern part of the Hexi Corridor since AD 1951. The precipitation reconstructions for other areas of the Hexi Corridor also demonstrated that a severe drought occurred in AD 1957 (Chen *et al.* 2011, 2013a). Rankings of the wettest and driest years in the eastern part of the Hexi Corridor in Table 3 show that AD 1957 was not only the driest year since AD 1951 but also the second driest year for the last 246 years in the eastern part of the Hexi Corridor. As shown in Table 3, five extremely dry years occurred in the 19th Century. However, the number of extremely dry years reached nine in the 20<sup>th</sup> Century. Additionally, ten of the wettest years occurred in the 20<sup>th</sup> Century, whereas only

**Table 2.** Calibration and verification statistics for the precipitation reconstruction.

	Calibration (1981–2010)	Verification (1951–1980)	Calibration (1951–1980)	Verification (1981–2010)	Full calibration (1951–2010)
$r$	0.664	0.677	0.677	0.664	0.664
$r^2$	0.441	0.458	0.458	0.441	0.441
RE		0.450		0.422	
CE		0.353		0.320	
Sign test		23 <sup>+</sup> /6 <sup>-</sup>		21 <sup>+</sup> /9 <sup>-</sup>	
First-order sign test		23 <sup>+</sup> /5 <sup>-</sup>		21 <sup>+</sup> /8 <sup>-</sup>	

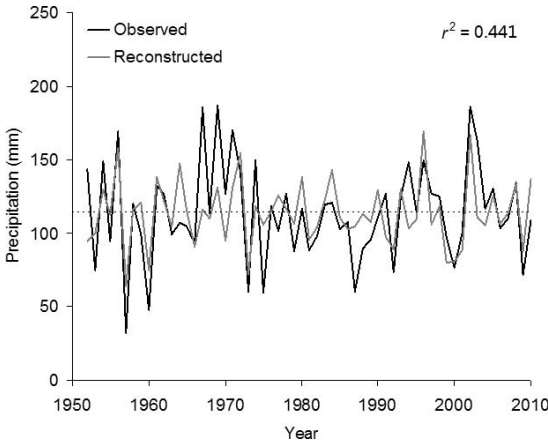


**Figure 4.** Comparison between observed and estimated precipitation from the previous August to the current May from 1951 to 2010.

seven extremely wet years occurred in the 19<sup>th</sup> Century. This indicated that more extreme climate events occurred in the 20<sup>th</sup> Century than in the 19<sup>th</sup> Century in the eastern part of the Hexi Corridor. As indicated by our precipitation reconstruction, the most severe and long-lasting droughts occurred in the 1870s–1880s and 1920s–1930s. These drought epochs resemble other findings in surrounding areas, suggesting the influence of large-scale droughts (Li *et al.* 2007; Liang *et al.* 2009; Chen *et al.* 2011, 2012, 2013, 2014a, 2015; Fang *et al.* 2012; Liu *et al.* 2013). In addition, the late 18<sup>th</sup> Century was reported as a drought epoch, with low precipitation and famine in western China (Yuan 1994).

Spectral analysis detected 9.3-, 6.7-, 3.1-, and 2.6-year periodicities in the reconstructed

**Table 3.** Rankings of the wettest and driest years in the eastern part of the Hexi Corridor from AD 1765 to 2010.

Rank	Dry year	Precipitation (mm)	Wet year	Precipitation (mm)
1	1833	61.0	1996	169.0
2	1957	63.8	2002	166.7
3	1767	69.8	1922	163.2
4	1973	72.3	1944	158.5
5	1928	74.1	1956	157.8
6	1884	74.2	1935	155.3
7	1960	74.9	1972	154.2
8	1947	76.1	1869	151.6
9	1940	77.5	1943	149.1
10	1999	80.1	1835	148.2
11	1779	80.7	1768	147.8
12	2000	80.7	1964	147.1
13	1819	82.4	1826	146.6
14	1798	83.3	1890	145.3
15	1799	83.6	1829	145.1
16	1930	84.6	1806	144.0
17	1855	86.1	1887	143.8
18	1848	86.5	1770	143.5
19	1931	86.5	1984	143.1
20	1878	86.6	1906	142.9

precipitation data for the eastern part of the Hexi Corridor (Figure 6). The 9.3-year cycle is likely related to the influence of solar forcing, and resembles other findings in surrounding areas (Li *et al.* 2007; Liang *et al.* 2009; Chen *et al.* 2012). Similarly, the 6.7-, 3.1-, and 2.6-year cycles fall within the range of variability of the El Niño–Southern Oscillation (ENSO) (Allan *et al.* 1996; Li *et al.* 2007). The climate of our study area is affected mutually by the Westerlies, Asian monsoon, and the interactions between the Tibetan Plateau and the Gobi Desert. Therefore, these cycles suggest the precipitation

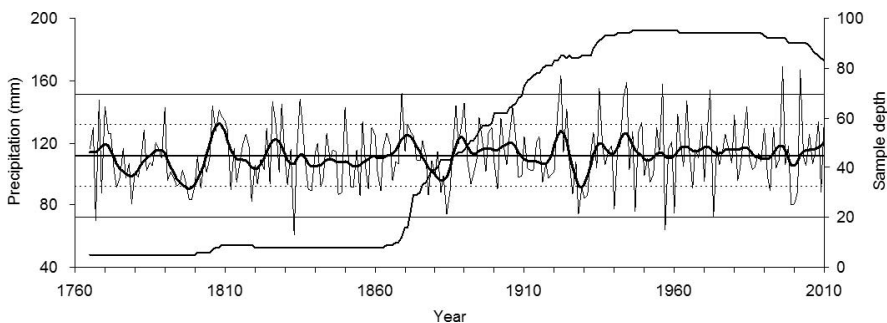


**Figure 5.** Estimated (thin line) and 10-year low-pass filter (thick line) values of total August–May precipitation for the eastern part of the Hexi Corridor. The central horizontal line shows the mean of the estimated values; the inner horizontal lines (dotted lines) show the border of one standard deviation, and the outer horizontal lines show two standard deviations.

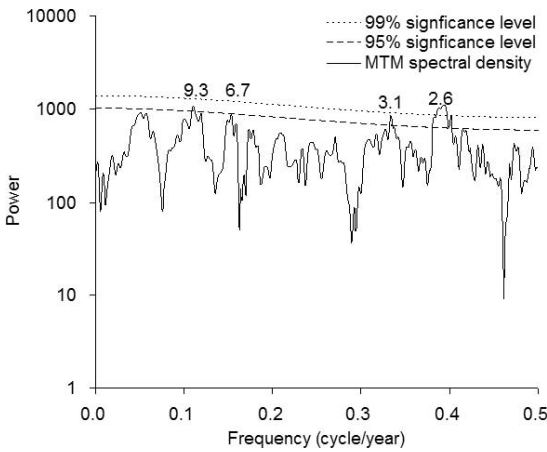


**Figure 6.** MTM spectral analysis results of the precipitation reconstruction. The dashed and dotted lines indicate the 95 and 99% significance level, respectively.

variation in the eastern part of the Hexi Corridor may have strong associations with large-scale atmospheric circulation.

### Regional Representativeness and Comparisons

To demonstrate the representativeness of the precipitation reconstruction for the eastern part of the Hexi Corridor, the reconstructed precipitation was compared with the precipitation dataset (New *et al.* 2000) using the KNMI climate explorer (<http://climexp.knmi.nl>) for the common period of 1951–2010. As shown in Figure 7, the actual (Figure 7a) and reconstructed (Figure 7b) precipitation series correlate significantly with the gridded

surface precipitation and show very similar spatial correlation fields. Significant positive correlations are found in the Hexi Corridor, with the highest correlations occurring in the eastern region. The results indicate that our precipitation reconstruction captures broad-scale regional precipitation variations and represents precipitation variations for a large territory in the Hexi Corridor.

Based on the moisture-sensitive tree-ring width series, the precipitation/drought series for five regions of Gansu Province, including Pingliang, Tianshui, Zhangye, Jiuquan and Lanzhou, have been reconstructed (Chen *et al.*, 2011, 2013a, 2013b, 2015; Fang *et al.* 2012). The studies also revealed that tree rings of spruce from relatively high altitude sites (>2300 m a.s.l.) in western and central Gansu mainly reflect annual (such as July–June) precipitation variation (Chen *et al.* 2011, 2013a, 2015), whereas tree rings of pine from eastern Gansu mainly reflect precipitation changes of the growing season (*i.e.* May–July) (Fang *et al.* 2012; Chen *et al.* 2013b). The cross-correlations of the precipitation/drought series in Table 4 show highly significant coefficients among the precipitation/drought series from the Hexi Corridor. Most of the correlation coefficients are significant at the 1% level. Despite spatial differences in local climate and tree growth and a complex mountainous terrain, the high positive correlations show that by using these precipitation/drought series, it is possible to create some wet/dry sequences that reflect regional-scale wet/dry variation. PCA revealed that the first principal components of the precipitation/

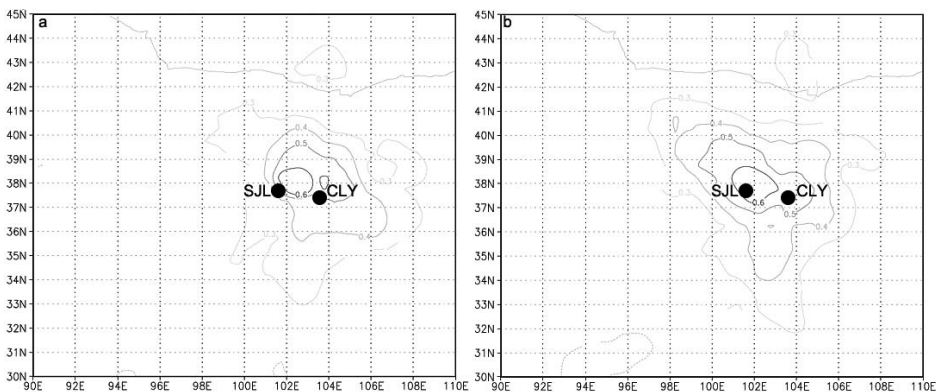


**Figure 7.** Spatial correlation fields of instrumental (a) and reconstructed (b) August–May precipitation for the eastern part of the Hexi Corridor with regional gridded August–May precipitation for the period of 1951–2010.

**Table 4.** Correlation matrix for tree-ring based precipitation/drought series from Gansu Province for the common time interval of 1816–2009.

	Tianshui	Lanzhou	Pingliang	Wuwei	Zhangye
Lanzhou	0.09				
Pingliang	0.41*	0.35*			
Wuwei	0.20*	0.37*	0.24*		
Zhangye	0.13	0.22*	0.19*	0.46*	
Jiuquan	0.11	0.29*	0.26*	0.31*	0.55*

\*Significant at  $p < 0.01$ .

drought series from western-central Gansu (PC#1<sub>w-c</sub>, Zhangye, Jiuquan and Lanzhou) and eastern Gansu (PC#1<sub>e</sub>, Pingliang and Tianshui) account for 70.63% and 52.63% of the total variance, respectively. The PC#1<sub>w-c</sub> compares well with PC#1<sub>e</sub>, with  $r = 0.31$  ( $n = 193$ ,  $p < 0.001$ ) on an annual scale and  $r = 0.38$  ( $p < 0.001$ , AD 1816–2008) on a decadal scale. The wet and dry periods in both curves are consistent on a decadal scale, demonstrating similar large-scale wet/dry variability (Figure 8). The two regions are influenced by the Asian summer monsoon. Thus, the synchronous variations in precipitation in the two regions reflect the strength of the variations of the Asian summer monsoon in Gansu.

Although similar trends between the records were found, many divergences between the two series were also detected in the 1810s–1820s, 1830s–1850, 1890s–1900s, 1940s–1950s and 1980s–1990s. In particular, a clear tendency towards a more arid climate has prevailed in Gansu since the 1980s, but the two regions have some differences

in terms of drought severity. This may be the out-of-phase relationship between the Asian summer monsoon and the Westerlies (Chen *et al.* 2008). The PC#1<sub>w-c</sub> not only includes the precipitation signals of the monsoon season but also includes the winter and spring precipitation signals. Tree growth at the high altitude sites benefits from the previous winter and early spring snow originating from the mid-latitude westerly flows, which increase the soil moisture content during the early part of the growing season. Conversely, the low altitude sites have relatively little winter and spring precipitation, and the low interannual variability of winter and spring precipitation lead to low response of pine growth. Although these seasonal precipitation reconstructions cannot capture the winter precipitation variability adequately because of tremendous impacts of growing-season precipitation on agricultural production, they still can provide hydroclimatic information for water resource planning and management.

## CONCLUSIONS

In this paper, a 246-year-long tree-ring based precipitation reconstruction from August to May in the eastern part of the Hexi Corridor was presented. The precipitation reconstruction reveals valuable information about severe drought events over the past 246 years, especially in the late 18<sup>th</sup> Century, the 1870s–1880s and the 1920s–1930s. The spectral analysis results indicate the existence of some important cycles for precipitation variability,

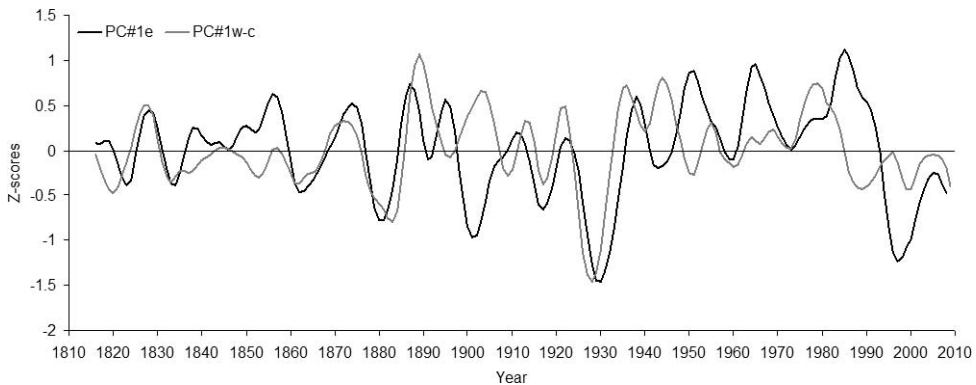


**Figure 8.** Comparison between the first principal components of the precipitation/drought series from western-central and eastern Gansu.

possible climatic mechanisms, and relationships with large-scale atmospheric circulation. Spatial correlation analysis indicates that our reconstruction represents a high degree of regional precipitation variability over the eastern part of the Hexi Corridor. Our precipitation also shows similar wet/dry periods to other reconstructed precipitation series of the Hexi Corridor.

PCA demonstrates that the PC1s is the appropriate record of the large-scale precipitation variability of western-central Gansu and eastern Gansu over the past 193 years. Based on the relationships between the Asian summer monsoon and the Westerlies, the precipitation variation in Gansu might also indicate a change in the Asian summer monsoon intensity. The analysis in this paper also suggests that water resource policies should not solely be based on individual site climate records, which have previously been used as references for regional water resource management. Large-scale reconstruction of hydroclimate variations should be considered by policy makers. Thus, to improve water resource planning, future studies using precipitation datasets of longer time spans and larger areas of spatial coverage are needed.

### ACKNOWLEDGEMENTS

This work was supported by the Meteorology Public Welfare Industry Research Special Project (GYHY201206014), China Desert Meteorological Science Research Foundation (Sqj2013015), NSFC Project (No. 41405081), and the Young Talent Plan of Meteorological Departments of China Meteorological Administration. We thank the anonymous reviewers for useful comments to improve the manuscript. We also thank Prof. Gou X.H. who kindly provided her data.

### REFERENCES CITED

- Allan, R. J., J. A. Lindesay, and D. E. Parker, 1996. *El Niño Southern Oscillation and Climatic Variability*. CSIRO Publishing, Clayton, Australia.
- Chen, F. H., Z. C. Yu, M. L. Yang, E. Ito, S. Wang, D. B. Madsen, X. Z. Huang, Y. Zhao, T. Sato, H. John, B. Birks, I. Boomer, J. Chen, C. An, and B. Wünnemann, 2008. Holocene moisture evolution in arid central Asia and its out-of-phase relationship with Asian monsoon history. *Quaternary Science Reviews* 27:351–364.
- Chen, F., Y. J. Yuan, and W. S. Wei, 2011. Climatic response of *Picea crassifolia* tree-ring parameters and precipitation reconstruction in the western Qilian Mountains, China. *Journal of Arid Environments* 75:1121–1128.
- Chen, F., Y. Yuan, W. S. Wen, S. Yu, Z. Fan, R. Zhang, T. Zhang, and H. Shang, 2012. Tree ring-based reconstruction of precipitation in the Changling Mountains, China, since A. D. 1691. *International Journal of Biometeorology* 56:765–774.
- Chen, F., Y. J. Yuan, W. S. Wei, R. B. Zhang, S. L. Yu, H. M. Shang, T. W. Zhang, L. Qin, H. Q. Wang, and F. H. Chen, 2013a. Tree-ring-based annual precipitation reconstruction for the Hexi Corridor, NW China: Consequences for climate history on and beyond the mid-latitude Asian continent. *Boreas* 42:1008–1021.
- Chen, F., Y. J. Yuan, W. S. Wei, Z. A. Fan, S. L. Yu, T. W. Zhang, R. B. Zhang, H. M. Shang, and L. Qin, 2013b. Reconstructed precipitation for the north-central China over the past 380 years and its linkages to East Asian summer monsoon variability. *Quaternary International* 283:36–45.
- Chen, F., Y. Yuan, R. B. Zhang, and L. Qin, 2014a. A tree-ring based drought reconstruction (AD 1760–2010) for the Loess Plateau and its possible driving mechanisms. *Global and Planetary Change* 122:82–88.
- Chen, F., H. Q. Wang, F. H. Chen, Y. J. Yuan, and R. B. Zhang, 2015. Tree-ring reconstruction of July–May precipitation (AD 1816–2010) in the northwestern marginal zone of the East Asian summer monsoon reveals the monsoon-related climate signals. *International Journal of Climatology* 35: 2109–2121.
- Cook, E. R., 1985. *A Time Series Analysis Approach to Tree-Ring Standardization*. Ph.D. thesis, University of Arizona, Tucson.
- Deng, Y., X. H. Gou, L. L. Gao, Z. Q. Zhao, Z. Y. Cao, and M. X. Yang, 2013. Aridity changes in the eastern Qilian Mountains since AD 1856 reconstructed from tree-rings. *Quaternary International* 80:379–393.
- Fang, K. Y., X. H. Gou, F. H. Chen, C. Z. Liu, N. Davi, J. B. Li, Z. Q. Zhao, and Y. J. Li, 2012. Tree-ring based reconstruction of drought variability (1615–2009) in the Kongtong Mountain area, northern China. *Global and Planetary Change* 80–81:190–197.
- Fritts, H. C., 1976. *Tree Rings and Climate*. Academic Press, London.
- Gou, X. H., Y. Deng, L. L. Gao, F. H. Chen, E. Cook, M. X. Yang, and F. Zhang, 2014. Millennium tree-ring reconstruction of drought variability in the eastern Qilian Mountains, northwest China. *Climatic Dynamics* doi:10.1007/s00382-014-2431-y.
- Holmes, R. L., 1983. Computer-assisted quality control in tree-ring dating and measurement. *Tree-Ring Bulletin* 43:69–95.
- Hughes, M. K., T. W. Swetnam, and H. F. Diaz, 2011. *Dendroclimatology: Progress and Prospects*. Springer Verlag, New York.
- Li, J., F. Chen, E. R. Cook, X. Gou, and Y. Zhang, 2007. Drought reconstruction for north central China from tree rings: The value of the Palmer drought severity index. *International Journal of Climatology* 27:903–909.
- Liang, E. Y., X. M. Shao, and X. H. Liu, 2009. Annual precipitation variation inferred from tree rings since AD 1770 for the western Qilian Mts., northern Tibetan Plateau. *Tree-Ring Research* 65(2):95–103.

- Liu, Y., Y. Lei, B. Sun, H. M. Song, and Q. Li, 2013. Annual precipitation variability inferred from tree-ring width chronologies in the Changling–Shoulu region, China, during AD 1853–2007. *Dendrochronologia* 31(4):290–296.
- Mann, M. E., and J. M. Lees, 1996. Robust estimation of background noise and signal detection in climatic time series. *Climatic Change* 33:409–445.
- Meko, D. M., and D. A. Graybill, 1995. Tree-ring reconstruction of Upper Gila River discharge. *Water Resources Bulletin* 31:605–616.
- New, M., M. Hulme, and P. Jones, 2000. Representing twentieth century space-time climate variability. Part II: development of a 1901–1996 monthly terrestrial climate field. *Journal of Climate* 13:2217–2238.
- Tian, Q. H., X. H. Gou, Y. Zhang, J. F. Peng, T. Chen, and J. S. Wang, 2007. Tree based drought reconstruction for the Qilian Mountains, northwestern China. *Tree-Ring Research* 63: 27–36.
- Wang, Q., J. A. Shi, G. J. Chen, and L. H. Xue, 2002. Environmental effects induced by human activities in arid Shiyang River basin, Gansu province, northwest China. *Environmental Geology* 43:219–227.
- Wang, B. J., Q. Zhang, and J. Zhang, 2004. Discussion about the environment degradation question of Minqin Oasis. *Arid Meteorology* (in Chinese) 22:87–92.
- Wigley, T., K. R. Briffa, and P. D. Jones, 1984. On the average value of correlated time series, with applications in dendroclimatology and hydrometeorology. *Journal of Climate and Applied Meteorology* 23:201–213.
- Yang, B., C. Qin, A. Bräuning, I. Burchardt, and J. Liu, 2011. Rainfall history for the Hexi Corridor in the arid northwest China during the past 620 years derived from tree rings. *International Journal of Climatology* 31:1166–1176.
- Yang, B., C. Qin, F. Shi, and D. M. Sonechkin, 2012. Tree ring-based annual streamflow reconstruction for the Heihe River in arid northwestern China from AD 575 and its implications for water resource management. *The Holocene* 22(7):773–784.
- Yuan, L., 1994. *Disaster and Famine history in Northwest China* (in Chinese). The People's Publishing Company of Gansu province, Lanzhou, China.

Received 19 October 2014; accepted 8 December 2015.